ADVANCED FUNCTIONAL MATERIALS
www.afm-journal.de

Layer-by-Layer Assembly of 3D Tissue Constructs with Functionalized Graphene

Su Ryon Shin, Behnaz Aghaei-Ghareh-Bolagh, Xiguang Gao, Mehdi Nikkhah, Sung Mi Jung, Alireza Dolatshahi-Pirouz, Sang Bok Kim, Sun Min Kim, Mehmet R. Dokmeci, Xiaowu (Shirley) Tang, and Ali Khademhosseini**

Carbon-based nanomaterials have been considered promising candidates to mimic certain structure and function of native extracellular matrix materials for tissue engineering. Significant progress has been made in fabricating carbon nanoparticle-incorporated cell culture substrates, but only a limited number of studies have been reported on the development of 3D tissue constructs using these nanomaterials. Here, a novel approach to engineer 3D multilayer constructs using layer-by-layer (LbL) assembly of cells separated with self-assembled graphene oxide (GO)-based thin films is presented. The GO-based structures are shown to serve as cell adhesive sheets that effectively facilitate the formation of multilayer cell constructs with interlayer connectivity. By controlling the amount of GO deposited in forming the thin films, the thickness of the multilayer tissue constructs could be tuned with high cell viability. Specifically, this approach could be useful for creating dense and tightly connected cardiac tissues through the co-culture of cardiomyocytes and other cell types. In this work, the fabrication of stand-alone multilayer cardiac tissues with strong spontaneous beating behavior and programmable pumping properties is demonstrated. Therefore, this LbL-based cell construct fabrication approach, utilizing GO thin films formed directly on cell surfaces, has great potential in engineering 3D tissue structures with improved organization, electrophysiological function, and mechanical integrity.

1. Introduction

The development of highly organized and functional 3D complex constructs in vitro is of great importance in tissue engineering, since native tissues and organs exhibit highly organized 3D complex architectures composed of extracellular matrix (ECM), different cell types, and chemical and physical signaling cues.[1,2] In particular, heart muscles are dense quasi-lamellar and highly vascularized tissues in which functional syncytia of the cardiomyocytes are tightly interconnected with gap junctions.[3,4] In recent studies, 3D biodegradable scaffolds, cell-embedded photocrosslinkable hydrogels or nano-/microfiberous scaffolds have shown significant potential for developing engineered 3D cardiac tissue.[5–7] Despite significant advances in this field, due to insufficient cell migration into scaffolds and limited

Dr. S. R. Shin, B. Aghaei-Ghareh-Bolagh,[+] Dr. M. Nikkhah,[++]
Dr. A. Dolatshahi-Pirouz, Dr. S. B. Kim, Dr. M. R. Dokmeci,
Prof. A. Khademhosseini
Biomaterials Innovation Research Center
Division of Biomedical Engineering
Department of Medicine
Brigham and Women's Hospital, Harvard Medical School
Cambridge, MA 02139, USA
E-mail: alik@rics.bwh.harvard.edu

Dr. S. R. Shin, B. Aghaei-Ghareh-Bolagh, Dr. M. Nikkhah,
Dr. A. Dolatshahi-Pirouz, Dr. S. B. Kim, Dr. M. R. Dokmeci,
Prof. A. Khademhosseini
Harvard-MIT Division of Health Sciences and Technology
Massachusetts Institute of Technology
Cambridge, MA 02139, USA

B. Aghaei-Ghareh-Bolagh
Department of Cell and Molecular Biology
Uppsala University
SE-751 24, Uppsala, Sweden

X. Gao, Prof. X. Tang
Department of Chemistry & Waterloo Institute for Nanotechnology
University of Waterloo
200 University Ave. West, Waterloo, Ontario N2L 3G1, Canada
E-mail: tangxw@uwaterloo.ca

Dr. S. M. Jung
Department of Electrical Engineering and Computer Science
Massachusetts Institute of Technology
Cambridge, MA 02139, USA

Dr. A. Dolatshahi-Pirouz
Interdisciplinary Nanoscience Center (iNANO)
Aarhus University
Aarhus, Denmark

Dr. S. M. Kim
Department of Mechanical Engineering
Inha University
Incheon 402-751, Republic of Korea

Dr. S. R. Shin, Dr. A. Dolatshahi-Pirouz, Dr. M. R. Dokmeci,
Prof. A. Khademhosseini
Wyss Institute for Biologically Inspired Engineering
Harvard University
Boston, MA 02115, USA

Prof. A. Khademhosseini
Department of Maxillofacial Biomedical Engineering
and Institute of Oral Biology
School of Dentistry, Kyung Hee University
Seoul 130-701, Republic of Korea

Prof. A. Khademhosseini
Department of Physics
King Abdulaziz University
Jeddah 21569, Saudi Arabia

[+]Present Address: Charles Perkins Centre D17, The University of Sydney, NSW 2006, Australia

[++]Present Address: School of Biological and Health Systems Engineering, Arizona State University, Tempe, AZ, 85287, USA

DOI: 10.1002/adfm.201401300

intercellular electrical coupling at gap junctions, mimicking the highly organized structure of myocardium with various types of cells still remains one of the major challenges in cardiac tissue engineering.[8]

Dense and highly organized 3D tissue constructs can be achieved by utilizing the layer-by-layer (LbL) assembly technique.[9] Several multilayer tissue constructs (blood vessels, skeletal muscle, and connective tissue) with well-controlled cellular type and location have been reported, where nanometer-thick films (nano-films) deposited on cell surfaces were used as the inter-layer spacer for the LbL assembly.[10,11] The physical and biological properties of the nano-films can be controlled by the type of ECM components (synthetic polymers, polysaccharides, poly-L-lysine (PLL),[9] fibronectin, and gelatin)[12,13] and the number of layers used in the thin films. To compensate for the limitations in conventional ECM materials' use in thin films, such as lack of electrical conductivity, nanoparticles with unique physical and chemical properties can be incorporated to create electrically active ECM like nano-films.[1] Recently, nanoparticles-incorporated hybrid hydrogels or solid substrates coated with nanoparticles were shown to improve the propagation of electrical signals and enhance cellular excitability by forming tight contacts with the cell membrane of both cardiomyocytes and neurons.[14–17] In addition, conductive nanoparticles were shown to promote cell attachment, growth, viability, differentiation and long-term survival of cells.[1,18,19] Therefore, we hypothesize that electrically active ECM-based nano-films may be used to engineer multilayer tissue constructs mimicking the morphological and electrophysiological features of native heart tissue.[1,20]

Here, we report the development of multilayer cell constructs using a LbL assembly technique by alternative cell seeding and nano-film deposition. The nano-films were formed by depositing PLL coated graphene oxide sheets (PLL-GO) directly onto pre-formed cell layers to facilitate cell separation and stacking. Graphene and its derivatives are known for their high electrical conductivity and strong mechanical properties. Specifically, GO has been used to prepare homogeneous aqueous suspensions in biological media. The presence of the oxygen-containing functional groups on the surface of GO can reduce the π–π stacking and van der Waals interactions between graphene sheets to prevent irreversible agglomeration. The nano-films made of PLL-GO possess voids allowing inter-cell layer connections and permeation of oxygen and nutrients, which are necessary to the creation of thick tissue constructs.[21,22]

It has recently been shown that GO has the ability to support attachment, growth, and differentiation of cells with little or no cytotoxic effects.[23,24] In previous studies, GO was shown to create smart 3D GO hydrogel as an active cell scaffold with high mechanical and electrical properties.[25–27] In addition, the cellular behavior on GO based materials can be regulated by tuning the surface oxygen content of GO.[28] Specially, the partially reduced GO have shown that the enhancement of stem cell adhesion and proliferation may be induced by enhanced ECM proteins adsorption on GO surface by non-covalent interactions. Furthermore, the shape of the nanoparticles determines the number and size of focal points/adhesions and therefore the strength of cell adhesion. Therefore, 2D GO might better promote cell adhesion and spreading compared to 1D carbon nanotubes or nanodiamonds. To improve the biological activity of GO, we decorated GO with PLL which is a polypeptide of the naturally occurring peptide L-lysine with excellent cell adhesive properties.[29,30] Therefore, bio-functionalization of GO particles by PLL is expected to provide a suitable cell-adhesive surface for the separation and formation of multilayers of cells. However, this thin layer of PLL will decrease the conductivity of GO at the beginning. However, the conductivity will be recovered after degradation of PLL, which is enzymatically biodegradable material. Furthermore, the use of PLL-functionalized GO could not only afford enhanced electrical connectivity between the different layers at biologically relevant frequencies but also adds mechanical strength to the multilayer tissue constructs due to the high mechanical strength of GO particles.[29,30]

2. Results and Discussion

2.1. Fabrication Process of 3D Multilayer Tissue Constructs Composed of Cells and PLL-GO

The fabrication of multilayer tissue constructs composed of cells and PLL-GO particles was performed according to the process illustrated in **Figure 1**a. The first step is to generate a stable and homogeneous cell layer as the bottom most layer. The second step is to deposit PLL-GO particles on the surface of the first cell layer which provides a cell-adhesive surface for the second layer of cells. Repetition of these two steps, i.e. LbL assembly, easily leads to tissue constructs with 3 or more cell layers.

Previous studies have relied on commercial semipermeable membranes,[10] or poly(vinylidene difluoride) membranes[31] as the primary substrates to create the LbL assembled tissue constructs due to their permeability to oxygen and nutrients, their ease of handling for cell culture, and harvestability of the cell sheets.[32] Although these substrates are suitable for the construction of LbL tissues, they lack the ability to regulate or enhance cellular behavior compared to the native tissue microenvironment. Therefore, a specifically designed substrate which can resemble the native ECM with similar mechanical, electrical, and biological properties will be very useful to create multilayer tissue constructs. Furthermore, it is highly preferable to have a substrate that is removable from the glass support after fabrication for clinical and device applications. To create biologically active substrates for the construction of LbL tissues, we selected substrates made of methacrylated gelatin (GelMA) hybrid hydrogels incorporated with carbon nanomaterials. In our previous studies, GO or CNT-embedded GelMA hybrid hydrogels with enhanced electrical conductivity and mechanical properties also had enhanced viability, elongation and proliferation of cells compared to those cultured on pristine GelMA hydrogels.[18,33] To evaluate the suitability of hybrid hydrogels as the primary substrates, 3T3 fibroblasts were seeded on GelMA, CNT-GelMA, and GO-GelMA hydrogel substrates with a typical thickness of 150 μm (Figure S1) and their behavior were subsequently monitored in real-time using a miniaturized microscope developed in our group.[34] Microscopic images captured at 20 min and 2 h after cell seeding

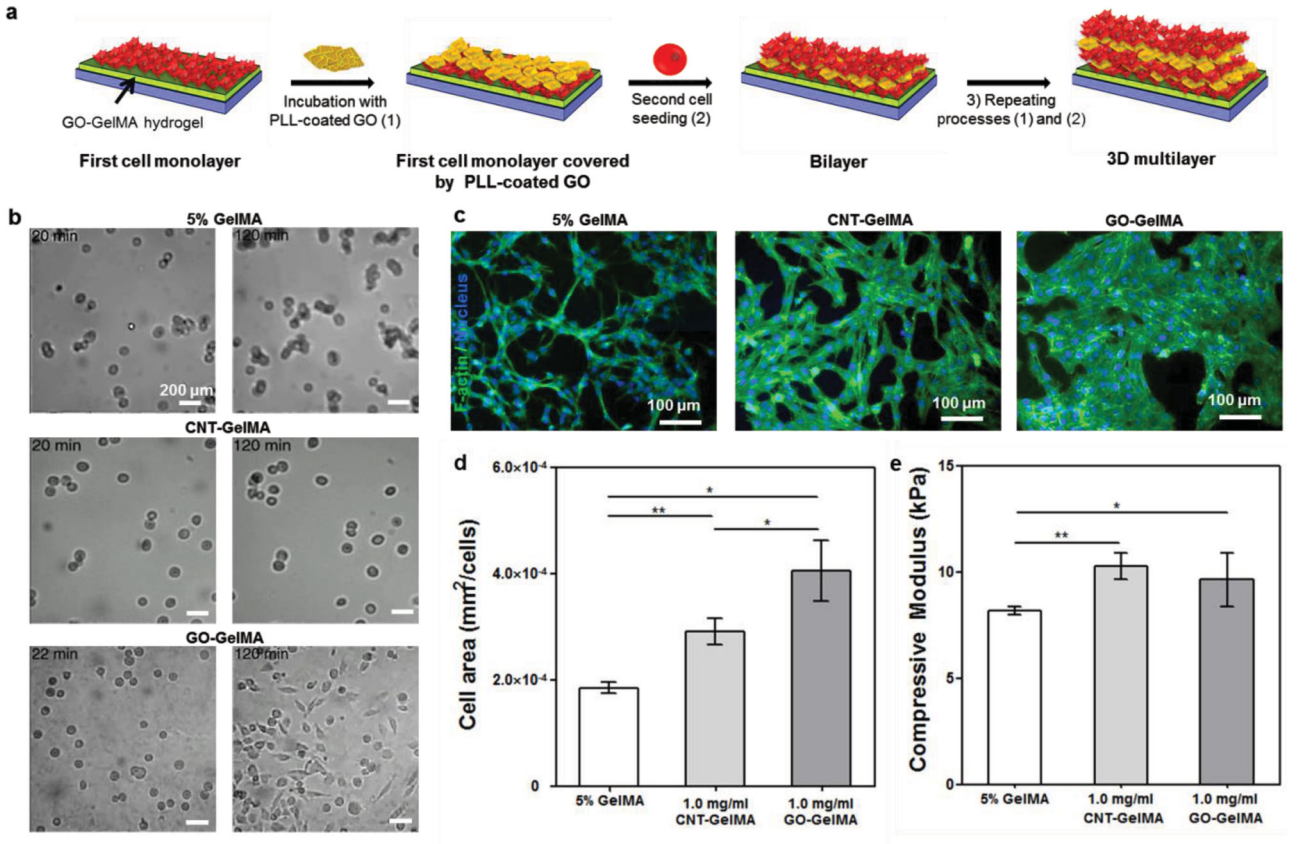

Figure 1. (a) Schematic illustration of the multilayer tissue constructs fabricated via LbL cell seeding and deposition of PLL-coated GO particles. (b) Images captured by a mini-microscope during adhesion and spread of 3T3 fibroblasts after they were seeded on 5% GelMA, CNT-GelMA (1.0 mg/mL), and GO-GelMA (1.0 mg/mL) hydrogel substrates. (c) Fluorescence images of 3T3 fibroblasts after 2-days of culture. F-actin and cell nuclei were labeled by green and blue fluorescent dyes respectively. (d) Cell size (i.e., area per cell) was generated by quantitative analysis of the fluorescence images. (e) The compressive modulus of pure GelMA, CNT-GelMA, GO-GelMA under compression at fully swollen state varied significantly with CNT concentration (*$p < 0.05$ and **$p < 0.001$).

showed that cells cultured on the GO-embedded GelMA substrates exhibited faster cell attachment, spreading and elongation than those cultured on CNT-GelMA and pristine GelMA hydrogel substrates (Figure 1b). Further, the cells seeded on GO-GelMA substrates displayed more homogeneous and well-interconnected planar polygon cellular shapes after 2 days of culture than those on CNT-GelMA and pristine GelMA surfaces (Figure 1c). The average cell size on GO-GelMA substrates was significantly larger than that on CNT-GelMA and pristine GelMA after 2 days of culture (Figure 1d). Interestingly, cell size and morphology on CNT-GelMA substrates were observed to be somewhat between those seeded on GO-GelMA and pristine GelMA surfaces. The cell morphology closely depends on substrate stiffness under conditions where chemical signals are constant.[35] Hence, we next analyzed the compression moduli of the three types of hydrogel substrates. However, the compressive modulus of the GO-GelMA gels is found to be similar to that of the CNT-GelMA gels (Figure 1e). Therefore, the difference between the morphology of 3T3 fibroblast cells on CNT- and GO-GelMA substrates might be related to the different geometrical shapes of these carbon nanoparticles rather than the overall gel stiffness. The shape of the nanoparticles determines the number and size of focal points/adhesions and therefore the strength of cell adhesion.[36] Although the exact mechanism of biological responses has not been fully elucidated, these results suggest that 2D GO nanoplatelets, compared to 1D carbon nanotubes, can promote cell adhesion and spreading. The use of GO-GelMA substrates allowed us to decrease the seeding time needed to ensure the adhesion and formation of a stable and homogeneously distributed first cell layer which is important to create the construction of LbL assembled tissue. Therefore, GO-GelMA substrates are used in the rest of this study to fabricate multilayered constructs.

2.2. PLL-GO Films

PLL-GO particles were deposited onto each cell layer to form a thin film, which functions similarly to an ECM for cell layer separation and binding. To create PLL-GO particles, an aliquot of a GO stock solution was mixed with a PLL solution and incubated at 37 °C for 1 h. The dispersed GO were then collected by centrifugation, washed several times to remove the excess PLL and resuspended in DPBS. To investigate the coating of GO by PLL, we performed zeta-potential measurements to analyze the surface charge on PLL-GO with various ratios of PLL to

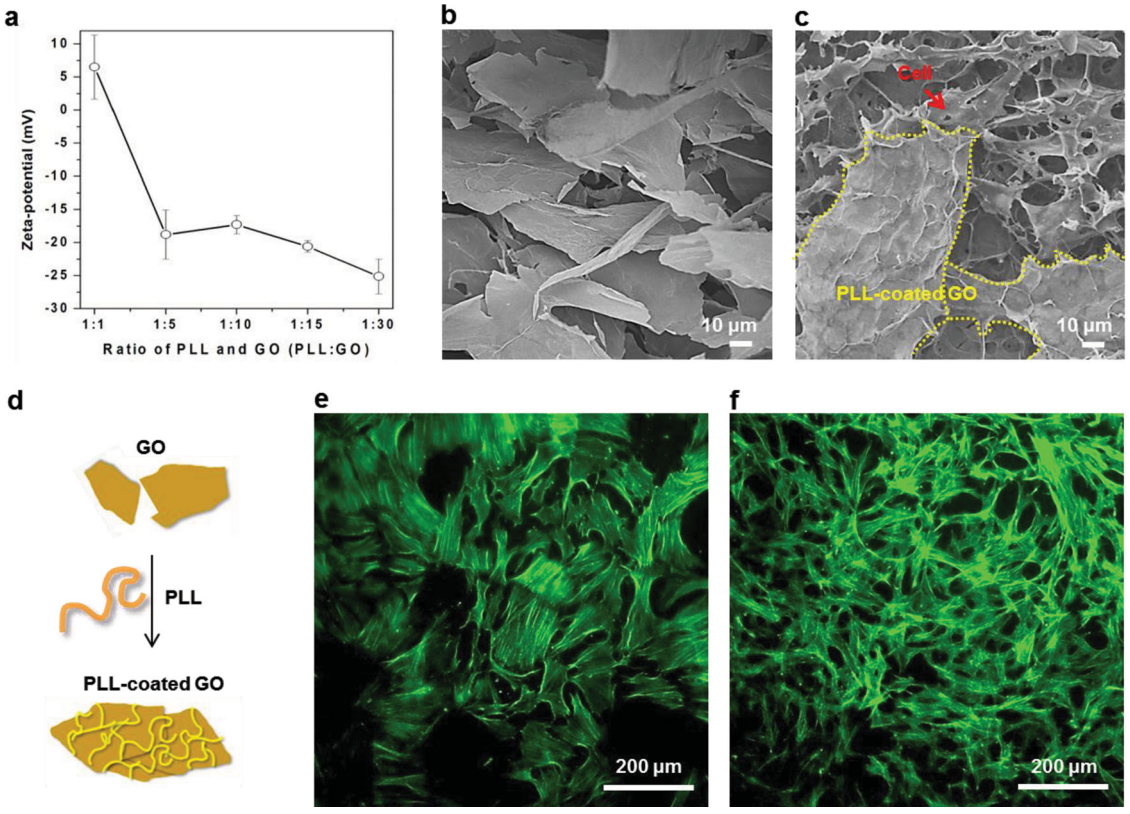

Figure 2. (a) Zeta potential analysis of different volume ratios of PLL: GO mixtures showing the surface charge of GO particles which were covered with different ratios of PLL. (b) A SEM image of the pristine GO particles and (c) PLL-coated GOs on the first 3T3 fibroblast mono layer after 10 min incubation at 37 °C. (d) Schematic diagram showing PLL coating onto the GO particles. The drawing is only a graphical representation and does not represent the precise means through which PLL polypeptide chains (yellow lines) interact with the GO surface. Fluorescent images of cultured hMSCs without (e) and with (f) a deposition of PLL-GO particles.

GO (**Figure 2**a). After PLL coating, the negatively charged GO showed a positive charge at 1:1 (GO:PLL) volume ratio where the viscosity of the GO solution was found to increase (Figure S2). The scanning electron microscopy (SEM) data shows the surface morphology between bare GO and PLL-GOs (Figure 2b and c). Compared to pristine GO (lateral size ~ 20 μm),[18] the PLL-GO displayed irregular shapes and larger size with lateral dimensions of up to ~100 μm, as shown in Figure 2c and Figure S3. This observation indicates that each PLL-GO particle consists of several pristine GO sheets crosslinked by a strong electrostatic attraction between negatively charged GO surfaces and positively charged PLL chains, as illustrated schematically in Figure 2d. In addition, partial covalent bonding between the free amine groups on PLL and the plentiful epoxy groups on GO may also contribute to the stable coating of PLL on GO.[30] This stable assembly of PLL-GO (outlined by yellow dotted line) deposited on 3T3 fibroblasts (red arrow) was observed by SEM imaging (Figure 2c). In order to elucidate the effect of PLL-GO particle deposition on cell morphology, PLL-GOs were deposited on the surface of the human mesenchymal stem cells (hMSCs) since hMSCs are known to display significantly different morphology depending on the microenvironment.[2] The PLL-GO induced highly elongated cell morphology, and consequently formed well-interconnected cellular networks that were visualized by immunofluorescence staining after 24 h of incubation (Figure 2e,f). Clearly, the formation of PLL-GO films directly on cell surfaces affected underlying hMSC cell morphology, which is likely attributed to the high stiffness of GO[37] and the condensation of polypeptide chains on the cell surface.[38,39] To assess the potential cytotoxicity of PLL-GO, a cell viability test was performed using the live/dead assay in the suspension of either bare or PLL-GO (Figure S4 and S5). No significant cytotoxicity was observed.

2.3. Fabrication of Multilayer Cell Constructs

To validate PLL-GO as a suitable interface material for tissue engineering, we fabricated 3 layer (3L) tissue constructs composed of 3T3 fibroblasts and PLL-GO films on a GO-GelMA hydrogel support substrate. Confocal laser scanning microscopy (CLSM) was employed to examine the thickness and morphology of the multilayer tissue constructs by staining the actin filament (F-actin) (green) and nuclei (blue) (**Figure 3**a and Figure S6). The 3L construct made with PLL-GO displayed a thicker tissue (~65 μm) compared to the construct without PLL-GO as a control (~23 μm). For the control sample, the second and third layers of cells were deposited on the surface of the first cell layer without a PLL-GO thin film. In Figure 3a, the thickness and size of the PLL-GO layers (empty black areas,

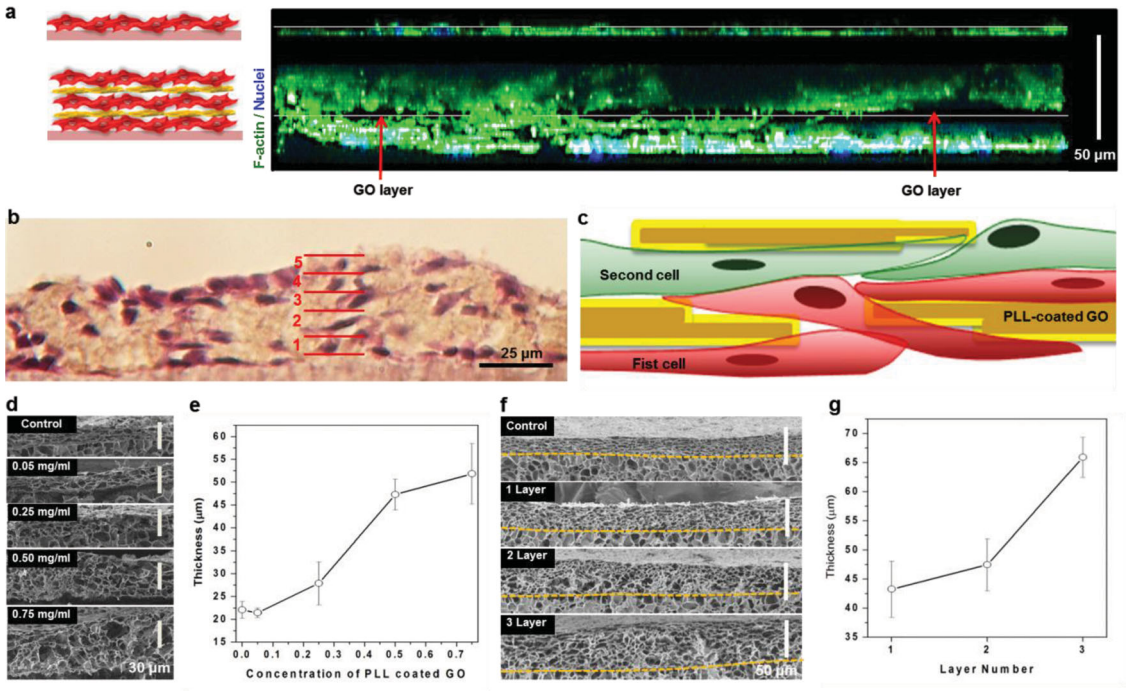

Figure 3. (a) Confocal cross-sectional images of the control group (top) and the 3L tissue constructs (bottom) after 2-days of culture. F-actin and cell nuclei were labeled with green and blue fluorescent dyes respectively. The 3T3 fibroblasts were found to connect the cells on the first layer to the cells on the second layer through non-continuous PLL-coated GO layer (red arrow, empty black area). (b) Hematoxylin and eosin (H&E) stain images of 3L 3T3 fibroblasts. The solid red lines indicate the interfaces between each layer. (c) Schematic illustration of the cross-section of the 2L construct showing the cells residing above and below the PLL-coated GO nanofilms. (d) SEM images showing the cross-section and (e) the thickness of 2L constructs fabricated with various concentrations of PLL-coated GOs as interlayer GO films. (f) SEM images showing the cross-section and (g) the thickness of 1L, 2L, and 3L constructs. The thickness of the constructs was estimated from the corresponding SEM images.

red arrows) were found to be in the range from a few microns to ~10 μm, which is much higher than that of the fibronectin (FN)-gelatin (G) nanofilms (6.2 nm).[12] To clearly identify the number of cell layers, haematoxylin and eosin (H&E) staining was performed to visualize the stacking of cells within the 3L construct (Figure 3b and Figure S7). Three to five layers of cells were observed to stack within the 3L tissue with a wavy layer-to-layer interface, which is similar to that reported in a previous study.[12] We suspect that the cells were interconnected by threadlike cytoplasmic prolongations through the gaps in between the PLL-GO particles or patches, created by discontinuities in the PLL-GO films, illustrated schematically in Figure 3c. Furthermore, the microscale holes might have contributed to the enhanced cell-cell communication and the permeability of the cellular construct to oxygen and nutrients.

To evaluate whether the thickness of the multilayer tissue construct could be controlled by varying the amount of PLL-GO deposited, we prepared 2-layer (2L) tissues with 400 μL of PLL-GO at various concentrations from 0 to 0.75 mg/mL (Figure 3d and e). The mean thickness of the obtained 2L constructs was estimated from cross-sectional SEM images. Thicker 2L tissues were obtained at higher PLL-GO concentrations due to the better cell stacking with homogeneously deposited PLL-GO compared to those of lower concentration of PLL-GO. The thickness plateaued at 51.8 ± 6.6 μm, with a PLL-GO concentration of 0.75 mg/mL, likely due to electrostatic repulsion between particles. For further experiments, 0.5 mg/mL was selected as the suitable concentration. In addition to changing the PLL concentration, the thickness of the tissue constructs can be controlled by increasing the number of layers. The mean thickness of 1L, 2L, and 3L cell assemblies was estimated to be 43.3 ± 4.8 μm, 47.4 ± 4.4 μm and 65 ± 3.4 μm respectively (Figure 3f and g). Interestingly, the PLL-GO-based multilayer tissues appeared to be thicker than the FN-GO-based multilayer constructs prepared by either LbL assembly (~25 μm, four layer construct) or the cell accumulation technique (~35 μm, approximately eight layer construct).[10] In addition, live/dead assays performed on the constructs showed excellent cell viability. To evaluate the cell populations inside the layers, an Alamar Blue assay was employed to measure the metabolic activity which showed a consistent increase in cell population as the number of layers increased (Figure S8). However, only cationic polypeptide (PLL), in which the electrostatic interaction is the only driving force for LbL assembly, have shown significantly different behavior of cells cultured inside the tissue construct. It was observed that cellular viability was found to decrease by increasing the number of layers due to the cytotoxicity of higher concentrations of the cationic polymer.[12] In previous studies, bio-functionalization of graphene substrates by coating them with ECM showed stronger cell attachment, higher cell viability and proliferation rate than ECM-coated gel substrates only.[23] It also supported a guided cell growth through the strong affinity between the nanomaterials and the ECM proteins and adsorbing certain proteins from the culture media.[39–41] Therefore, we expect that the positively charged PLL-GO can effectively provide a cell-adhesive surface

between the first and the second layer with no cytotoxic effects through both electrostatic interactions and strong cell adhesion. Furthermore, we noticed that the discontinuous hybrid PLL-GO films enable strong cell-cell coupling between different layers. This tight interconnections formed between cells is important for cardiac applications which mediate the reciprocal exchange of small molecules and ions resulting in synchronized beating of cell clusters. These factors are important in creating a stably organized 3D cardiac tissue with functional syncytia of cardiomyocytes.

2.4. Multilayer Cardiac Constructs

We next demonstrated the generation of multilayer cardiac tissues using the LbL assembly of cardiac and endothelial cells (ECs) with PLL-GO thin films facilitating cell separation and support (**Figure 4**a and b). The organization of cardiomyocytes and ECs into a multilayer tissue was investigated after 5 days of culture. CLSM of F-actin (green) labeled cardiomyocytes/ECs and CD-31 (red) labeled ECs showed that the spatial organization of 2L or 3L tissues were successfully controlled by alternating the seeding order of cells and PLL-GOs (Figure 4a). The ECs were found to be homogeneously distributed and showed network formation in the multilayer tissues (Figure 4b and Figure S8). In contrast, when ECs were deposited on a cardiomyocyte layer without PLL-GO (Figure 4a (i)) or with only a PLL interlayer (Figure 4a (ii)), a heterogeneous monolayer was observed.

We next demonstrated the advantages of PLL-GO in the fabrication of functional multilayer cardiac tissue constructs. In Figure 4c, the 2L cardiomyocyte/cardiac fibroblast tissue with PLL-GO as the interlayer residing on a GO-GelMA substrate was robust enough to be peeled off from the glass slide. On day 3, the maturation of cardiomyocytes in 2L tissues was assessed using immunofluorescence staining of the cardiac specific marker sarcomeric α-actinin (red). The 2L cardiac tissue exhibited well-developed and interconnected sarcomeric structures in Figure 4c. Also, 1L, 2L, and 3L tissue constructs composed of cardiac fibroblasts and cardiomyocytes were successfully obtained with a thickness of ~11, 33 and 52 μm, respectively (Figure S9). In previous studies, carbon nanomaterials have been reported to guide cell–cell interactions and to facilitate cellular organization, and to promote cell maturation.[16,42] The fabricated tissues, both 2L cardiomyocyte/ECs and cardiomyocyte/cardiac fibroblasts, demonstrated strong spontaneous and synchronous beating behavior (~20 or 30 beats per min (BPM)) only after one day of culture. When a 2L cardiomyocyte/cardiac fibroblast tissue (square shape, 1 cm^2) was detached from the glass slide, it would spontaneously form

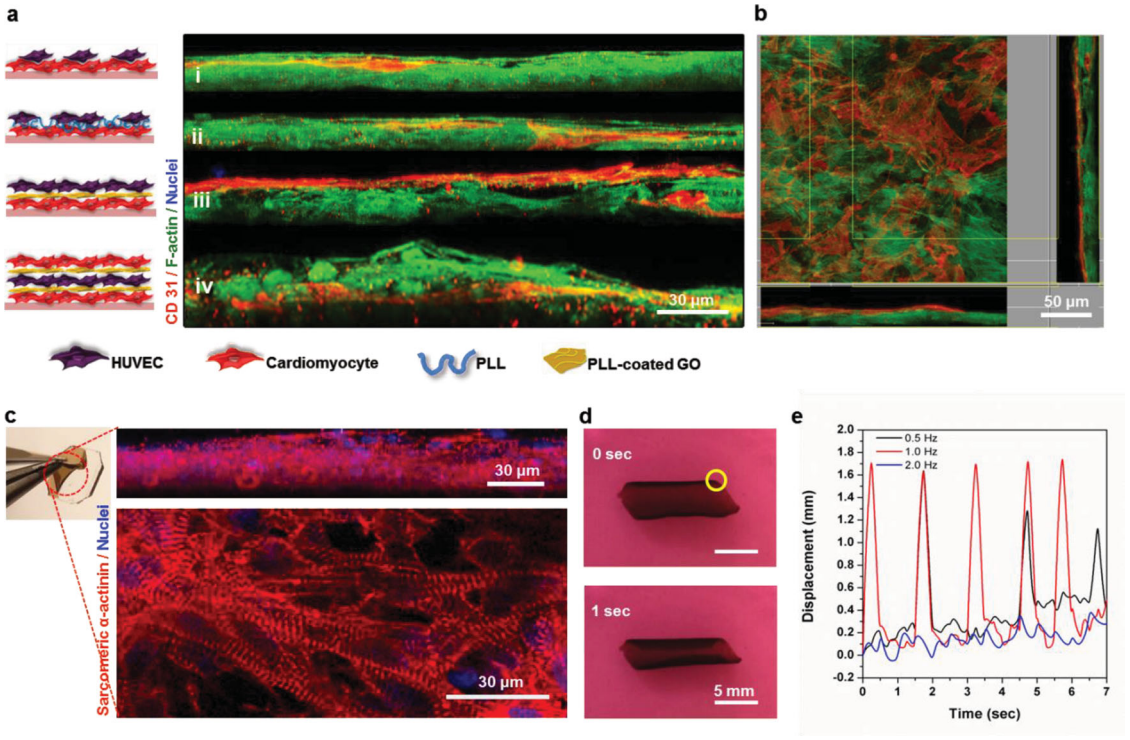

Figure 4. (a) Schematic illustration (left) and 3D reconstructed confocal cross-section images (right) of 2L cardiomyocytes and ECs without any ECM layers (i), with pristine PLL (ii), with PLL-coated GOs (iii), and 3L cardiomyocytes and ECs with PLL-coated GOs (iv) as the interface layers between cells. Cardiomyocytes and ECs were stained with phalloidin (green), ECs were immunostained with CD31 (red) and the nuclei were stained with DAPI (blue) after 5-days of culture. (b) Confocal images (top view) of sample (iii) showing widespread EC networks. (c) A photograph of the peeling process of cellular construct and the confocal images of the interconnected sarcomeric structures (top image: cross-section; bottom image: top view) of the 2L cardiomyocyte construct after 3-days of incubation. The cardiac cells were immunostained with sarcomeric α-actinin (red) and nuclei with DAPI (blue). (d) Optical images of the 2L cardiac actuator. (e) Displacement of the actuator (focusing on the tip inside the yellow circle in (d)) over time under electrical stimulation (Square wave, 1.4 V/cm, Frequency: 0.5–2 Hz, Pulse width: 50 ms).

a loosely rolled-up tubular shape in culture medium without shrinking (Figure 4d). In previously studies, cardiomyocyte cell sheets shrunk when detached from temperature-responsive surfaces by reducing temperature due to cytoskeletal tensile reorganization.[43] In addition, the released 2L cardiac tissues still showed strong spontaneous synchronous beating immediately after detachment (SI, Movie 1). In comparison, it takes a few days for the cardiomyocyte cell sheets prepared by temperature-responsive polymer to recover their beating behavior after release from the substrate. This actuator (total thickness: ~210 μm) with electrically stimulated opening/closing motion is similar to our previously reported pumping actuator fabricated on CNT-GelMA films (thickness ~ 100 μm) (SI, Movie 2).[14] In addition, this frequency-dependent actuation (0.5, 1, and 2 Hz) can be controlled by applying a low external electric field (1.4 V/cm) as shown in Figure 4d,e. These results suggest that multilayer 3D cardiac tissues have great potential as biohybrid actuators, similar to the previously reported 2D cardiac tissue actuator on CNT incorporated GelMA and FN-coated polydimethylsiloxane films.[44,45] In comparison, 2L cardiac tissue without PLL-GO could not generate a strong beating behavior (SI, Movie 3). The overall enhanced contraction function of the multilayer cardiac tissue with PLL-GO could result from a combination of several factors. First, the presence of PLL-GO generated dense cardiomyocyte tissue construct and promoted cardiomyocyte maturation, as indicated by the strong expression of sarcomeric α-actinin. The second is the enhanced cell-cell communications by forming tightly connected and organized cell networks between different layers. Last, by bridging the cells, the GO particles provided additional pathways for reducing the impedance between cells which facilitated the charge distribution and propagation of action potentials. Similar mechanism was proposed to boost neuronal signaling by CNTs in a previous study.[16]

3. Conclusions

Multilayer tissues were successfully fabricated by using a LbL assembly technique where PLL-GO thin films were deposited as an adhesive layer in between each cell layer and facilitated the assembly through electrostatic attraction and strong cell adhesion. Our approach started with seeding cells onto a thin GO-GelMA hybrid hydrogel substrate (150 μm), which was of vital importance to ensure a stable and homogeneous bottom cell layer. Then, a buffered solution of PLL-GO was then deposited onto each cell layer to form the adhesive film. PLL-GO were made by coating GO particles with PLL through strong electrostatic attractions between the PLL and GO. The architecture of the multilayer cell construct was successfully controlled by the concentration of the PLL-GO, the number of stacked layers and the cell type and location. Compared to previously reported tissue constructs, our approach generated multilayer tissues with enhanced biological activity, mechanical integrity, ease of handling, and retrievability of engineered tissue. Cardiomyocytes, ECs, and hMSCs inside our multilayer constructs showed a high level of cell viability, elongation and proliferation. Multilayer cardiac tissue fabricated by seeding cardiomyocytes between PLL-GO showed strong spontaneous beating and frequency-dependent opening/closing actuation under a low external electric field. Our results indicate that the PLL-GOs embedded within the multilayer cardiac constructs improved cardiac cell organization, maturation, and cell-cell electrical coupling. Therefore, nanoparticles combined with a LbL stacking approach presented here offers a novel technique for the engineering of electrically propagating complex tissues.

4. Experimental Section

Preparation of GO-GelMA and CNT-GelMA Hydrogels: GelMA was synthesized based on previously reported procedures.[46] To prepare GelMA prepolymer solution, lyophilized GelMA (5 wt%) and photoinitiator (0.5 wt%), 2-hydroxy-1-(4-(hydroxyethoxy) phenyl)-2-methyl-1-propanone (Irgacure 2959; CIBA chemical), were dissolved in DPBS at 80 °C for 30 min. Next, CNT-GelMA hybrid hydrogels (1.0 mg/mL) were prepared based on our previously published results.[14] GO was prepared from graphite according to modified Hummer's method and has wide range of size distribution (area on the order of 10–18 000 nm^2).[18,47] GO dispersion in water was then added to the GelMA solution (5%) containing 0.5% photoinitiator at 80 °C to prepare prepolymer solution containing 1.0 mg/mL GO nanoparticles. To fabricate UV-crosslinked GO-GelMA hydrogel substrates, 20 μL of the prepolymer solution was pipetted in between two glass slides separated by a 150 μm spacer and subsequently covered with 3-(trimethoxysily) propyl methacrylate (TMSPMA) coated glass slide (Figure S1). The prepared prepolymer solutions were exposed to UV light at 6.9 mW /cm^2 (360-480 nm) for 5 s (5% GelMA), 25 s (1.0 mg/mL GO-GelMA), and 50 s (1.0 mg/mL CNT-GelMA) to obtain substrates with a dimension of 1 cm (width) × 1 cm (length) × 150 μm (thickness).

Scanning Electron Microscopy (SEM): Hydrogels were exposed to DPBS overnight so they reached their fully swollen state. After freezing at –80 °C and lyophilizing, they were cut from the middle to expose their cross-section. The cross-section and the surface of the hydrogels were sputter coated by Pt/Pd and the detailed structure and morphology of pores were investigated by a SEM (Hitachi Model S4700, Japan).

Indentation: To measure the elastic modulus of the hydrogel films, swollen samples in DPBS with a thickness of 150 μm were tested on a Nano-UTM (Nano-bionix) machine. All the tests were carried out using a spherical indenter with a radius of 1 mm to generate a maximum load of 0.3 mN at an approaching rate of 0.1 μm/s. The sample size was 3 films per group.

Cell Adhesion Experiment using the Mini-Microscope Imaging System: 3T3 fibroblasts were cultured at 5% CO_2 atmosphere and 37 °C in high glucose Dulbecco's Modified Eagle Medium (DMEM) supplemented with 10% FBS and 1% penicillin-streptomycin. The cells were passaged twice a week. To study the effect of carbon nanoparticles on cell attachment and spreading, the cells (5.0×10^4 cell/well) were seeded on hydrogel-based substrates. Behavior of cells was monitored for 12 h inside a 37 °C incubator using a mini-microscope developed in our lab.[34] Images were captured at different time points (20 min and 2 h) to compare the cell behavior on different substrates.

Preparation and Characterization of PLL-Coated GO Particles: To prepare positively charged PLL-coated GO particles (PLL-GO), an aqueous dispersion of GO was mixed with PLL solutions with different V/V ratios of PLL and GO (1:1, 1:5, 1:10, 1:15 and 1:30). The mixtures were then sonicated for 30 min at room temperature (DEGAS, power 9 mW). After 1 h incubation in PLL solution at 37 °C, the dispersed PLL-GO particles were collected by centrifugation and washed several times to remove unreacted PLL (5000 RPM, 5 min). All samples were re-suspended in PBS to a final volume of 1 mL and the surface charge on pristine GO and PLL-GO particles was measured using zeta potential (ZEN3600 zetasizer, Malvern Instruments).

PLL-Coated GO Toxicity Test: To assess the cytocompatibility of GO and PLL-GO particles, 3T3 fibroblast cells (5.0×10^4 cell/well) were

seeded in 24-well plates and incubated at 37 °C overnight to adhere to the tissue culture wells. PLL-GO particles with 1:1 ratio of PLL to GO were prepared in a similar procedure mentioned in the previous section. The obtained PLL-GO particles was diluted with fresh media to the target concentrations of 0, 5, 50 and 500 μg/mL GO. Pristine GO and PLL coated GOs suspended in fresh media were deposited on adhered cells and incubated at 37 °C for 48 h. Live/dead assay was performed to evaluate the cellular viability. Proliferation of incubated cells with these particles (0, 0.1, 1, 10, 100 and 1000 μg/mL) was evaluated with an MTS assay according the manufacturer's instructions.

Preparation of 3D Multilayer Tissue Constructs: To fabricate the first cell monolayer, 3T3 cells (1.0×10^6 cell/mL) were seeded on the surface of GO-GelMA hydrogel (1.0 mg/mL) substrate. After 3 h of incubation at 37 °C, unattached cells were washed away and the prepared cell monolayer was incubated with PLL-GO particles for 30 min. Unreacted PLL-GO particles were washed away by fresh media. To prepare 2L constructs, the second layer of cells were seeded on top of the PLL-GO layer. Unattached cells were washed after 3 h incubation at 37 °C and the second layer of PLL-GO was then deposited on the surface of cells. After overnight incubation, unattached particles were removed and the process was repeated one more time to fabricate the 3L constructs. In order to optimize the concentration of nanoparticle layer, PLL-GO solutions with different concentrations of GO particles (0.0, 0.05, 0.25, 0.5, 0.75 mg/mL) were prepared. 2L constructs with different concentrations of nanoparticles were prepared and cultured for 5 days. Upon fixation in 2.5% glutaraldehyde, the samples were freeze-dried and their cross-sections were imaged by SEM. Based on the initial results, 0.5 mg/mL PLL-GO was selected as the suitable concentration for the remainder of the experiments. To measure the thickness of 1L, 2L and 3L constructs, all samples were cultured for 5 days and prepared for SEM imaging by fixation in 2.5% glutaraldehyde and subsequent freeze-drying.

Characterization of Multilayer 3D Constructs: Live/dead assay (Invitrogen, USA) was performed using calcein-AM (for live cells) and ethidium homodimer (for dead cells) according to the manufacturer's instructions. Samples were incubated with assay solutions for 30 min at 37 °C and imaged using an inverted fluorescence microscope (Nikon, Eclipse TE 2000U, Japan). Alamar Blue proliferation assay was performed to measure the metabolic activity of cells inside the assembled cellular constructs according to the manufacturer's instructions. Immunostaining of cells was performed using Phalloidin/DAPI staining of F-actin/Nuclei. Samples were washed by DPBS, and fixed using 4% paraformaldehyde (PFA) for 20 min at room temperature. After washing with DPBS, the cells were permeabilized to dyes by incubation with 0.1 % triton X -100 for 30 min. Samples were incubated for 45 min with Alexa Fluor 488 phalloidin and DAPI, at 1:40 and 1:1000 dilutions in DPBS, respectively. After washing with DPBS, the stained cells were imaged using an inverted CLSM (Leica SP5X MP, Germany). For histology studies, samples were fixed by 4% PFA for 20 min at room temperature. After washing with DPBS, the constructs were immersed in 30% sucrose and incubated at 4 °C overnight. Then the samples were snap-frozen by embedding them in medium (Tissue-Tek O.C.T compound) and cut into 10 μm thick sections. The sections were mounted on slides and stained with haematoxylin and eosin (H&E).

Preparation of Constructs with hMSCs: Bone marrow-derived hMSCs were cultured in Minimum Essential Medium Alpha (MEM-α) supplemented with 10% heat-inactivated FBS and 1% penicillin-streptomycin in a 5% CO_2 atmosphere at 37 °C. The cells were cultured until 70% confluence and used before passage 5. The hMSCs (7.5×10^4 cell/mL) were seeded on GO-GelMA hydrogels (1.0 mg/mL) and incubated at 37 °C overnight (control). To prepare a mono layer sample, PLL-GOs were deposited on the prepared cell layer and incubated for 2 h at 37 °C. Unreacted nanoparticles were washed with media and after 5 days of the culture, control and the mono layer samples were immunostained for F-actin by phalloidin and then imaged using a fluorescent microscope.

Cell Isolation and Culture: Neonatal rat ventricular cardiomyocytes were isolated from 2-day-old Sprague-Dawley rats following a well-established protocol approved by the Institute's Committee on Animal Care.[14] Cardiomyocytes were used immediately after their isolation and enrichment through 1 h pre-plating to separate cardiac fibroblasts. Cardiomyocytes was harvested from the supernatant media. Cardiac fibroblasts were cultured until 90% confluence in DMEM (Gibco, USA) containing 10% FBS (Gibco, USA), 1% L-Glutamine (Gibco, USA) and 100 units/mL penicillin-streptomycin (Gibco, USA). Cardiac fibroblasts were trypsinized and obtained. The multilayer samples were cultured in cell culture media up to 5 days without electrical stimulation.

Statistical Analysis: Statistical analysis was performed using one-way or two-way ANOVA methods to define the level of significance (GraphPad Prism 5.02, GraphPad Software). Tukey's multiple comparison tests were used to determine whether a significant difference existed between different conditions.

Supporting Information

Supporting Information is available from the Wiley Online Library or from the author.

Acknowledgements

S. R. Shin and B. Aghaei-Ghareh-Bolagh contributed equally to this work. X. Tang and A. Khademhosseini also contributed equally to this work. This work was supported by the Institute for Soldier Nanotechnology, National Institutes of Health (HL092836, EB02597, AR057837, HL099073), the National Science Foundation (DMR0847287), the Office of Naval Research Young Investigator award and ONR PECASE Award, and the National Research Foundation of Korea Grant funded by the Korean Government (NRF-2010-220-D00014). A. Dolatshahi-Pirouz was supported by the Danish Council for Independent Research (Technology and Production Sciences, 10-100118).

Received: April 22, 2014
Revised: May 31, 2014
Published online: July 31, 2014

[1] T. Dvir, B. P. Timko, D. S. Kohane, R. Langer, *Nat. Nanotechnol.* **2011**, *6*, 13.
[2] M. P. Lutolf, P. M. Gilbert, H. M. Blau, *Nature* **2009**, *462*, 433.
[3] G. C. Engelmayr Jr., M. Cheng, C. J. Bettinger, J. T. Borenstein, R. Langer, L. E. Freed, *Nat. Mater.* **2008**, *7*, 1003.
[4] T. Eschenhagen, A. Eder, I. Vollert, A. Hansen, *Am. J. Physiol.: Heart Circ. Physiol.* **2012**, *303*, H133.
[5] R. Gauvin, A. Khademhosseini, *ACS Nano* **2011**, *5*, 4258.
[6] P. Zorlutuna, N. Annabi, G. Camci-Unal, M. Nikkhah, J. M. Cha, J. W. Nichol, A. Manbachi, H. Bae, S. Chen, A. Khademhosseini, *Adv. Mater.* **2012**, *24*, 1782.
[7] R. Ravichandran, J. R. Venugopal, S. Sundarrajan, S. Mukherjee, S. Ramakrishna, *Tissue. Eng. Part. A* **2011**, *17*, 1363.
[8] B. Liau, D. Zhang, N. Bursac, *Regen. Med.* **2012**, *7*, 187.
[9] M. Matsusaki, H. Ajiro, T. Kida, T. Serizawa, M. Akashi, *Adv. Mater.* **2012**, *24*, 457.
[10] A. Nishiguchi, H. Yoshida, M. Matsusaki, M. Akashi, *Adv. Mater.* **2011**, *23*, 3506.
[11] O. Guillame-Gentil, O. Semenov, A. S. Roca, T. Groth, R. Zahn, J. Voros, M. Zenobi-Wong, *Adv. Mater.* **2010**, *22*, 5443.
[12] M. Matsusaki, K. Kadowaki, Y. Nakahara, M. Akashi, *Angew. Chem.* **2007**, *119*, 4773.
[13] H. Hosoya, K. Kadowaki, M. Matsusaki, H. Cabral, H. Nishihara, H. Ijichi, K. Koike, K. Kataoka, K. Miyazono, M. Akashi, M. R. Kano, *Biochem. Biophys. Res. Commun.* **2012**, *419*, 32.

[14] S. R. Shin, S. M. Jung, M. Zalabany, K. Kim, P. Zorlutuna, S. B. Kim, M. Nikkhah, M. Khabiry, M. Azize, J. Kong, K. T. Wan, T. Palacios, M. R. Dokmeci, H. Bae, X. S. Tang, A. Khademhosseini, *ACS Nano* **2013**, *7*, 2369.
[15] E. Mooney, J. N. Mackle, D. J. Blond, E. O'Cearbhaill, G. Shaw, W. J. Blau, F. P. Barry, V. Barron, J. M. Murphy, *Biomaterials* **2012**, *33*, 6132.
[16] G. Cellot, E. Cilia, S. Cipollone, V. Rancic, A. Sucapane, S. Giordani, L. Gambazzi, H. Markram, M. Grandolfo, D. Scaini, F. Gelain, L. Casalis, M. Prato, M. Giugliano, L. Ballerini, *Nat. Nanotechnol.* **2008**, *4*, 126.
[17] T. Dvir, B. P. Timko, M. D. Brigham, S. R. Naik, S. S. Karajanagi, O. Levy, H. Jin, K. K. Parker, R. Langer, D. S. Kohane, *Nat. Nanotechnol.* **2011**, *6*, 720.
[18] S. R. Shin, B. Aghaei-Ghareh-Bolagh, T. T. Dang, S. N. Topkaya, X. Gao, S. Y. Yang, S. M. Jung, J. H. Oh, M. R. Dokmeci, X. S. Tang, A. Khademhosseini, *Adv. Mater.* **2013**, *25*, 6385.
[19] C. Cha, S. R. Shin, N. Annabi, M. R. Dokmeci, A. Khademhosseini, *ACS Nano* **2013**, *7*, 2891.
[20] J. O. You, M. Rafat, G. J. Ye, D. T. Auguste, *Nano Lett.* **2011**, *11*, 3643.
[21] J. Hong, N. J. Shah, A. C. Drake, P. C. DeMuth, J. B. Lee, J. Chen, P. T. Hammond, *ACS Nano* **2012**, *6*, 81.
[22] R. R. Nair, H. A. Wu, P. N. Jayaram, I. V. Grigorieva, A. K. Geim, *Science* **2012**, *335*, 442.
[23] X. Shi, H. Chang, S. Chen, C. Lai, A. Khademhosseini, *Adv. Funct. Mater.* **2012**, *22*, 751.
[24] G. Y. Chen, D. W. Pang, S. M. Hwang, H. Y. Tuan, Y. C. Hu, *Biomaterials* **2012**, *33*, 418.
[25] W. Li, J. Wang, J. Ren, X. Qu, *Adv. Mater.* **2013**, *25*, 6737.
[26] H. N. Lim, N. M. Huang, S. S. Lim, I. Harrison, C. H. Chia, *Int. J. Nanomed.* **2011**, *6*, 1817.
[27] Y. Wang, W. C. Lee, K. K. Manga, P. K. Ang, J. Lu, Y. P. Liu, C. T. Lim, K. P. Loh, *Adv. Mater.* **2012**, *24*, 4285.
[28] X. Shi, H. Chang, S. Chen, C. Lai, A. Khademhosseini, H. Wu, *Adv. Funct. Mater.* **2012**, *22*, 751.
[29] K. Zhou, G. A. Thouas, C. C. Bernard, D. R. Nisbet, D. I. Finkelstein, D. Li, J. S. Forsythe, *ACS Appl. Mater. Interfaces.* **2012**, *4*, 4524.
[30] C. Shan, H. Yang, D. Han, Q. Zhang, A. Ivaska, L. Niu, *Langmuir* **2009**, *25*, 12030.
[31] H. Obokata, M. Yamato, S. Tsuneda, T. Okano, *Nat. Protoc.* **2011**, *6*, 1053.
[32] T. Sasagawa, T. Shimizu, S. Sekiya, Y. Haraguchi, M. Yamato, Y. Sawa, T. Okano, *Biomaterials* **2010**, *31*, 1646.
[33] S. R. Shin, H. Bae, J. M. Cha, J. Y. Mun, Y.-C. Chen, H. Tekin, H. Shin, S. Farshchi, M. R. Dokmeci, X. Tang, A. Khademhosseini, *ACS Nano* **2012**, *6*, 362.
[34] S. B. Kim, K. I. Koo, H. Bae, M. R. Dokmeci, G. A. Hamilton, A. Bahinski, S. M. Kim, D. E. Ingber, A. Khademhosseini, *Lab Chip* **2012**, *12*, 3976.
[35] M. Guvendiren, J. A. Burdick, *Nat. Commun.* **2012**, *3*, 792.
[36] S. R. Ryoo, Y. K. Kim, M. H. Kim, D. H. Min, *ACS Nano* **2010**, *4*, 6587.
[37] A. J. Engler, S. Sen, H. L. Sweeney, D. E. Discher, *Cell* **2006**, *126*, 677.
[38] M. Abdul Kafi, W. A. El-Said, T. H. Kim, J. W. Choi, *Biomaterials* **2012**, *33*, 731.
[39] S. Namgung, T. Kim, K. Y. Baik, M. Lee, J. M. Nam, S. Hong, *Small* **2011**, *7*, 56.
[40] M. Abdul Kafi, W. A. El-Said, T. H. Kim, J. W. Choi, *Biomaterials* **2012**, *33*, 731.
[41] K. Y. Baik, S. Y. Park, K. Heo, K. B. Lee, S. Hong, *Small* **2011**, *7*, 741.
[42] V. Martinelli, G. Cellot, F. M. Toma, C. S. Long, J. H. Caldwell, L. Zentilin, M. Giacca, A. Turco, M. Prato, L. Ballerini, L. Mestroni, *Nano Lett.* **2012**, *12*, 1831.
[43] T. Shimizu, M. Yamato, Y. Isoi, T. Akutsu, T. Setomaru, K. Abe, A. Kikuchi, M. Umezu, T. Okano, *Circ. Res.* **2002**, *90*, e40.
[44] A. W. Feinberg, A. Feigel, S. S. Shevkoplyas, S. Sheehy, G. M. Whitesides, K. K. Parker, *Science* **2007**, *317*, 1366.
[45] J. C. Nawroth, H. Lee, A. W. Feinberg, C. M. Ripplinger, M. L. McCain, A. Grosberg, J. O. Dabiri, K. K. Parker, *Nat. Biotechnol.* **2012**, 792.
[46] J. W. Nichol, S. T. Koshy, H. Bae, C. M. Hwang, S. Yamanlar, A. Khademhosseini, *Biomaterials* **2010**, *31*, 5536.
[47] W. S. Hummers, R. E. Offeman, *J. Am. Chem. Soc.* **1958**, *80*, 1339.